Four Separate Dimensionless Collisionality Scans in various JET Scenarios

T. Tala[1], H. Nordman[2], A. Salmi[1], D. Tegnered[2], C. Bourdelle[3], P. Carvalho[4], A. Czarnecka[5], L. Giacomelli[4], C. Giroud[6], E. Belonohy[6], J. Hillesheim[6], C. Maggi[6], P. Mantica[4], M. Maslov[6], L. Meneses[7], S. Menmuir[5], S. Mordijck[8], V. Naulin[9], J. Juul Rasmussen[9], G. Sips[10], M. Tsalas[11], H. Weisen[12] and JET contributors*

EUROfusion Consortium, JET, Culham Science Centre, Abingdon, OX14 3DB, UK
[1]VTT, P.O. Box 1000, FI-02044 VTT, Espoo, Finland
[2]Chalmers University of Technology, Gothenburg 41296, Sweden
[3]CEA, IRFM, F-13108 Saint-Paul-lez-Durance, France
[4]Istituto di Fisica del Plasma, via Cozzi 53, 20125 Milano, Italy
[5]IPPLM, Warsaw, Poland
[6]CCFE, Culham Science Centre, Abingdon, OX14 3DB, UK
[7]Instituto de Plasmas e Fusão Nuclear, IST, Universidade de Lisboa, Portugal, IST, Lisbon, Portugal
[8]College of William & Mary, Virginia, USA
[9]Danish Technical University Physics, Lyngby, Denmark
[10]Commission, Brussels, Belgium
[11]DIFFER, Nieuwegein, Netherlands
[12]SPC, Lausanne, Switzerland
*See the author list of Litaudon et al, "Overview of the JET results in support to ITER", Nucl. Fusion, **57** 102001 (2017).

1. Introduction

Particle transport in tokamaks has received much less attention than electron and ion heat transport channels. It is still often not treated self-consistently in transport modelling and predictions for future tokamaks. As a consequence, particle transport and fuelling remain one of the major open questions in understanding the ITER physics [1]. The shape of the density profile has a significant influence on fusion performance and impurity transport.

Particle transport has been extensively studied by performing several dimensionally matched collisionality scans in various plasma scenarios in JET. Gas puff modulation technique has been developed with high quality time-dependent density profile measurements to determine particle transport coefficients on JET [2]. The local electron density response to the gas injection was measured Thomson scattering diagnostics close to the midplane. Modulation amplitudes below 0.3-0.5% at mid-radius are reliably measured thus allowing minimal plasma disturbance and the possibility to use data from multiple harmonics. The gas puff modulation was performed with a gas valve at the top of the machine at 3Hz frequency using rectangular waveform, the rate varying from 0 to $6x10^{22}s^{-1}$ at 30% duty cycle.

2. Dimensionless Collisionality Scans in Various JET Plasmas

The following 4 separate and independent 3-point υ* scans were performed in JET: (i) high power ELMy H-mode featuring low β, (ii) hybrid like high β H-mode plasma, (iii) ELMy H-mode plasma in Hydrogen and (iv) L-mode with carbon wall. The dimensionless parameters, q, ρ^*, β_n and T_i/T_e (being very close to 1 in each of the scans presented here) were typically matched very well, the difference between the shots being only a few % (<10% in worst case). The density profiles from the 4 different dimensionless 3-point collisionality scans with respect to density peaking are presented in figure 1. The density profile is measured with Thomson scattering diagnostics and averaged over the stationary phase of the discharge, typically of the order of more than 5s (except in Hybrid-like plasmas). The error bars of these time averaged profiles are small, of the order of a few %. The collisionality υ* or alternatively υ_{eff} is varied simultaneously by a factor of roughly 5 within each scan. Unlike in all the different scans with H-mode plasma edge (executed with ITER-like-wall), no change in density peaking factor was observed in L-mode (carbon wall). The results from both of the dedicated H-mode and L-mode scans are consistent with the earlier density peaking database

results in L-mode [3] and H-mode [4,5]. Recently, the baseline H-mode scan (i) was experimentally repeated in JET by running as long stationary plasma discharges as possible (up to 13s stationary phase) and collecting gas puff modulation data. The steady-state profiles give the same dependence of the density peaking on υ* as that in figure 1 (upper left frame).

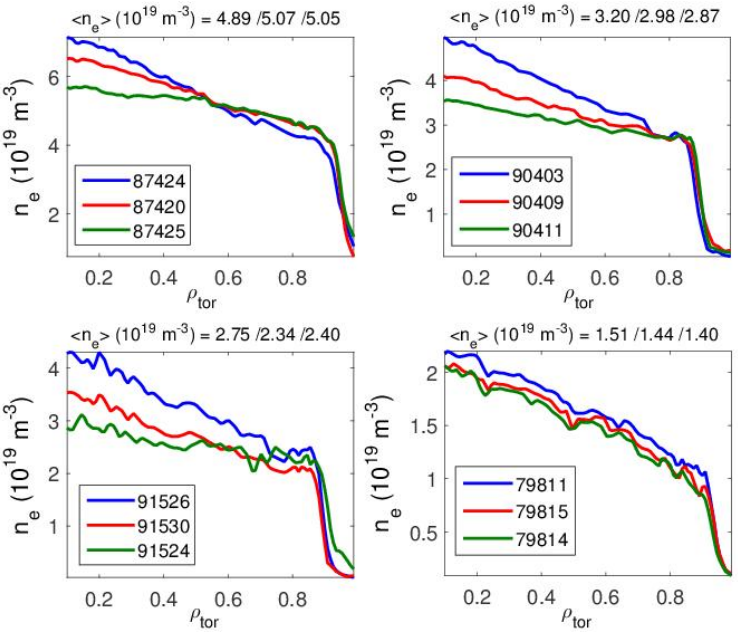

Figure 1. Density profiles from the following four different dimensionless collisionality scans: (top left, case (i)) high power ELMy H-mode featuring low β, (top right, case (ii)) hybrid like high β plasma, (bottom left, case (iii)) ELMy H-mode plasma in Hydrogen and (bottom right, case (iv)) L-mode with carbon wall. The blue colour refers to the low collisionality case, the green one to high collisionality (red intermediate).Profiles time averaged over long period of time ~10s.

3. Experimental Determination of the Particle Transport Coefficients

The analytical expressions for the diffusion coefficient D and particle pinch v are obtained from the approach based on perturbative particle transport equation, modulated density data and stationary background transport [6]. The equations in this paper are modified to include the real JET geometry. The particle source is negligible inside ρ<0.8, probably even ρ<0.9.

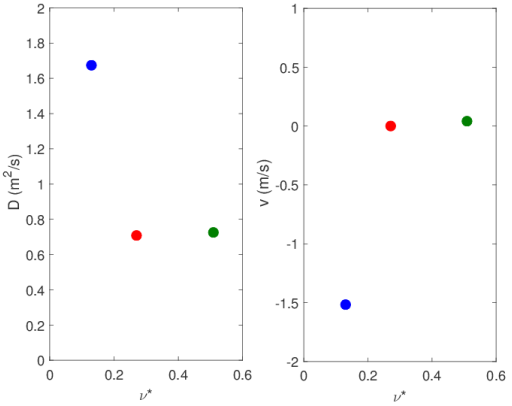

Figure 2. The experimental D and v for the baseline scan (colours correspond to the ones in upper left frame in figure 1). The data is averaged from ρ=0.55 up to ρ=0.8.

The conclusion from this υ* scan is that D increases as a function power as expected and at higher and also at intermediate υ*, the pinch is practically non-existent. At lower υ*, the pinch starts to play a significant role but even for that discharge, the NBI fueling is responsible for significant part of the observed density peaking. The high and intermediate υ* (red and green) shots have small uncertainties ~30% as they are long shots, 12-13s, and have 35 modulation cycles, but the low υ* point has larger uncertainty ~50%, at least the convection velocity v. D has quite small uncertainty also for that discharge.

4. Transport and Gyro-kinetic Simulations of the Collisionality Scans

In order both to validate particle transport models and codes against this excellent set of data and to obtain further clarification on the relative role of NBI fueling versus inward pinch in contributing to core density peaking, numerous transport and gyro-kinetic simulations have been performed. The models used so far in the analysis are GLF23 and QuaLiKiz and GENE code for GK runs. Predictive simulations of T_i, T_e, n_e and interpretative v_{tor} and q (boundary values adopted at ρ=0.8-0.85).

The transport simulation results are summarized in figure 3 for the Deuterium baseline scan discharge at lowest collisionality (blue curves in figure 1m upper left corner). GLF23 is in good agreement with the experimental observation on density peaking, predicting some short 50% of the peaking from NBI fueling and the other good 50% from the inward pinch. The predictions for the middle and high collisionality cases are very similar to this in terms of density peaking. The corresponding modelling results in the L-mode scan are in line with the results of the baseline scan below; GLF23 are in good agreement with experiment, but NBI fueling plays a smaller role in L-mode. QuaLiKiz underpredicts the density peaking.

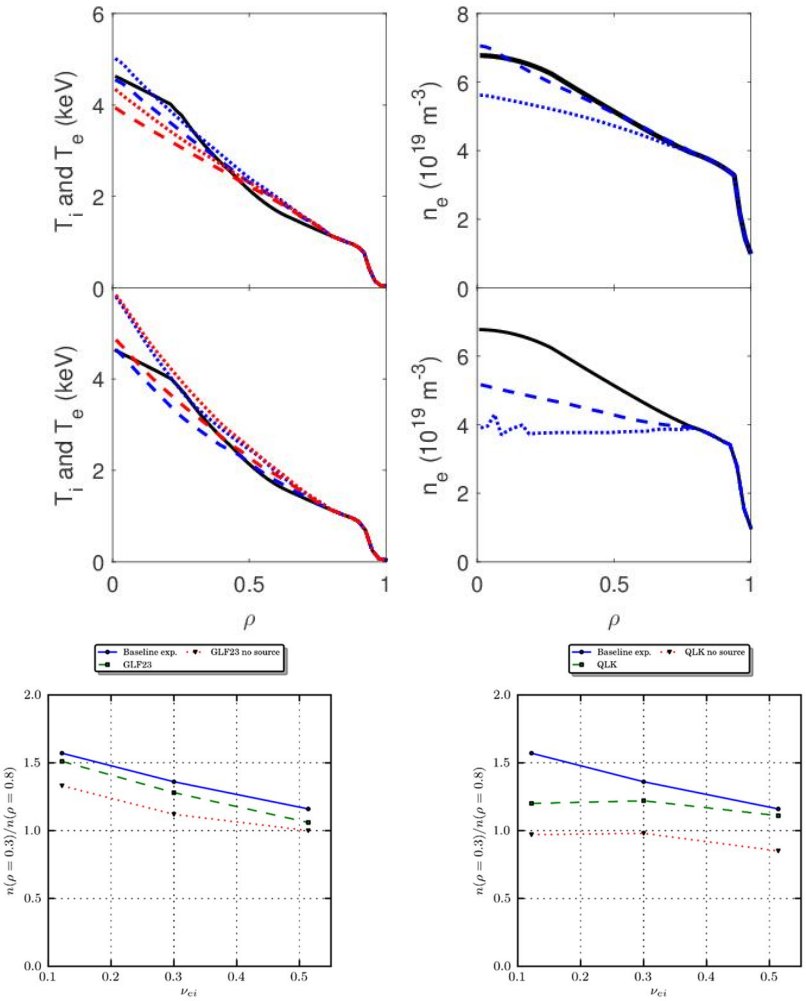

Figure 3. The predictions from GLF23 (upper row) and QuaLiKiz (middle row) against experimental data (black solid curves) with NBI particle source (dashed) and without it (dotted) for the low collisionality discharge. The ion temperature prediction is marked with blue and electron with red colour. The bottom row compares the experimental and predicted global peaking factors using the data from the baseline scenario 3-point scan.

The GENE simulations were performed to find the density gradient of zero particle flux to infer the peaking factor of background ions in the absence of sources at ρ=0.6 and ρ=0.8. The peaking factor (PF) is defined as $PF = R/L_n = -RV/D$ which is found by performing scans in R/L_n and finding $\Gamma/q = 0$. The linear and nonlinear simulations of ITG/TE mode turbulence at

kρ=0.2 were performed in flux tube domain, with a realistic geometry, including finite β_e effects and collisions using a Landau-Boltzmann collision operator, but excluding fast particles and impurities.

The GENE results at kρ=0.2 yield peaked density profiles only for L-mode. All H-modes and hybrids discharges give hollow density profiles at ρ=0.6 while at ρ=0.8 are moderately peaked for some cases, still the peaking for all 9 H-mode shots is underpredicted, similarly to QuaLiKiz predictions. Similar peaking factor trends within each scan with and without collisions are found, but the actual peaking factor is higher without the collisions.

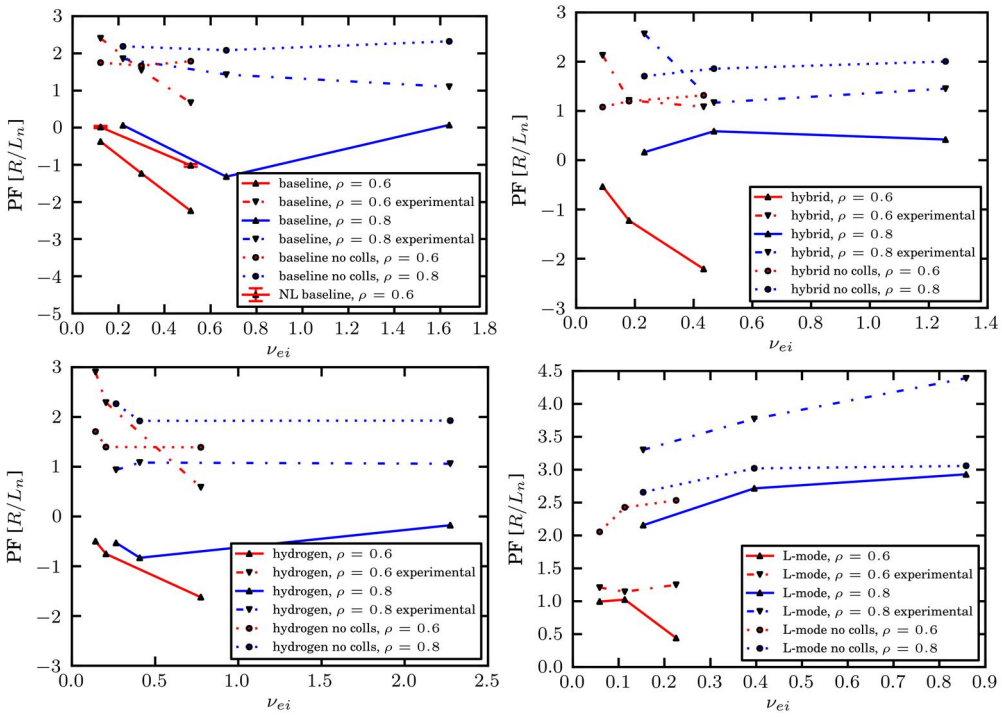

Figure 4. The GENE simulation results for the 4 separate collisionality as in figure 1 (the frames in the same order).

5. Conclusions

The experimental evidence shows that in all these H-mode scans, NBI fueling plays a significant role in contributing to density peaking. At high collisionality, NBI fueling is responsible for more than half of the peaking. This experimental evidence is supported by both the transport simulations and GENE runs, which both tend to assign even larger role for the NBI fueling. The new results with gas puff modulation data, allowing the experimental determination of D and v, are in line with earlier work in Refs. [7,8]. The key questions here to remain are how these results extrapolate to ITER at lower collisonality and if some other parameter than collisionality becomes important in the extrapolation.

Acknowledgement: "This work has been carried out within the framework of the EUROfusion Consortium and has received funding from the Euratom research and training programme 2014-2018 under grant agreement No 633053. The views and opinions expressed herein do not necessarily reflect those of the European Commission."

[1] A. Loarte *et al.*, Nucl. Fusion **53**, 083031 (2013).
[2] T. Tala et al., 26th IAEA Fusion Energy Conf. 17-22 October 2016, (Kyoto, Japan, 2016), paper EX/P6-12.
[3] H. Weisen et al., Plasma Phys. Control. Fusion **46**, 751 (2004).
[4] H. Weisen *et al.*, Plasma Phys. Control. Fusion **48**, A457 (2006).
[5] C. Angioni *et al.*, Nucl. Fusion **47** 1326–1335 (2007).
[6] H. Takenaga et al., Plasma Phys. Control. Fusion **40**, 193 (1998).
[7] M. Valovic et al., PPCF 46, 1877 (2004).
[8] L. Garzotti et al., Nucl. Fusion 46, 994 (2006).